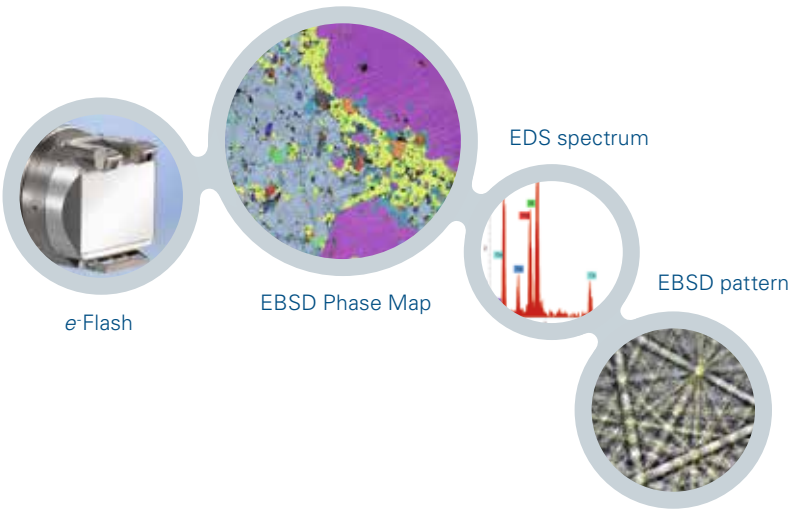

Application Note # EBSD-03

Phase identification and distribution on a mineralogical sample

In the last decade, the EBSD technique has evolved - thanks to its combination with EDS - from being a tool for texture quantification to a complete microstructure characterization method. It is now more systematically used for quantifying grain size, phase distribution, grain boundary analysis and phase identification. EBSD analysis has become a standard analytical tool in Earth Sciences.

Limitations can arise when the specimen contains several phases. However, phases with similar chemical compositions but different crystallographic structures can be distinguished by EBSD, whilst EDS discriminates phases with similar crystallographic structures but of different chemical compositions. Using a specimen which contains both types of phases, it can be demonstrated that simultaneous measurement and combined processing of EDS and EBSD data can overcome these limitations.

This application example reveals the benefit of the Advanced Phase Identification (ID) feature of the Bruker ESPRIT software for the characterization of a complex mineralogical sample. Not only does Advanced Phase ID assist in finding all the phases in a semi-automated procedure, it also improves indexing quality by determining the best fitting phase out of nearly 500,000 entries from the available databases (ICSD - regularly updated, AMCSD, COD, Bruker).

Methodology

Manual phase identification via optical microscope or SEM is time-consuming, laborious, and the quality of its results is user-dependent. These pitfalls are avoided with the use of Bruker's Advanced Phase ID.

This software feature employs the automated collection of a chemical spectrum via EDS, as well as corresponding crystallographic orientation via EBSD for every point analyzed. Combining chemical and crystallographic information allows accurate phase(s) identification and increases indexing rate and measurement accuracy when compared to analysis with manually detected phases.

Missed phases can also be identified offline using the Advanced Phase ID procedure and ultrafast re-indexing, without need of additional time on the SEM.

In addition, the robust indexing algorithm of the ESPRIT software and the automatic selection of reflectors for each phase prevent misindexing between the numerous low and high crystal symmetries phases, as typically encountered in geologically formed mineralogical samples.

Sample

The sample shown in Fig. 1 is a multiphase mineralogical sample of an oceanic oxide gabbro. It was collected from an Oceanic Core Complex and has been sampled during the Integrated Ocean Drilling Program Expedition 304/305 from Hole U1309D.

Atomic contrast image

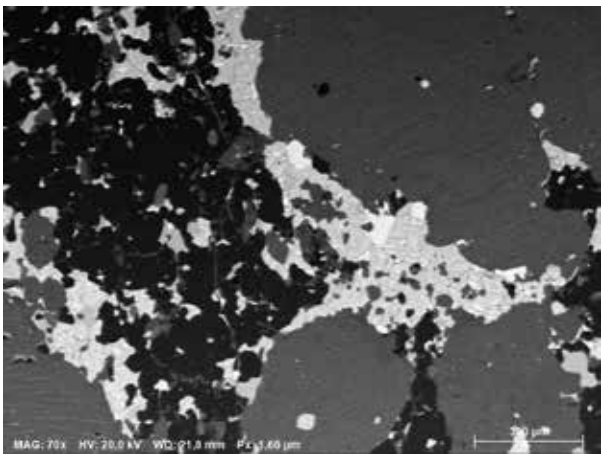

Fig. 1 ARGUS™ BSE image of the measured area. It shows the "chemical contrast" in grayscale.

The sample 137R-2-40 was extracted from the center of a 9 cm wide oxide gabbro intrusion in section U1309D-137R-2 located at 679 m depth. The bulk of this core section is amphibole bearing gabbro which exhibits greenschist facies alteration and serpentinization. The modal mineralogy of the thin section consists of 55% feldspar, 25% pyroxene, 10% opaques, and 10% alteration phases (talc, tremolite, and chlorite).

The ARGUS™ atomic contrast image in Fig. 1 reveals the complexity of the phase distribution in the sample. From this image the presence of at least four different phases and fine exsolutions can be inferred.

The sample is a standard 30 µm mechanically polished thin section with a final stage using 0.04 µm colloidal silica.

Measurement conditions

A simultaneous EBSD/EDS measurement of the sample was performed with a Bruker QUANTAX system consisting of an XFlash® detector with 30 mm^2 active area and an *e*$^-$Flash HR$^+$ EBSD detector.

- Acceleration voltage: 20 kV
- Probe current: ~ 7 nA
- Exposure time: 12 ms
- Reanalysis speed: 280 pps (8:04 min)
- Total map size: 1658 x 1244 $µm^2$
- EBSP resolution: 160 x 120 pixels
- Hit rate: 94.3%
- Average grain size: 41 µm

Online Advanced Phase ID

Prior to running the automated combined EBSD/EDS measurement, one phase was identified by the following procedure:

1. Acquisition of an EDS spectrum and a diffraction pattern (EBSP) at the same position (Fig. 2).
2. The databases were searched for candidate phases based on the major elements in the EDS spectrum (containing Fe and O). In this analysis it results in 384 possible phases.

Phase identification

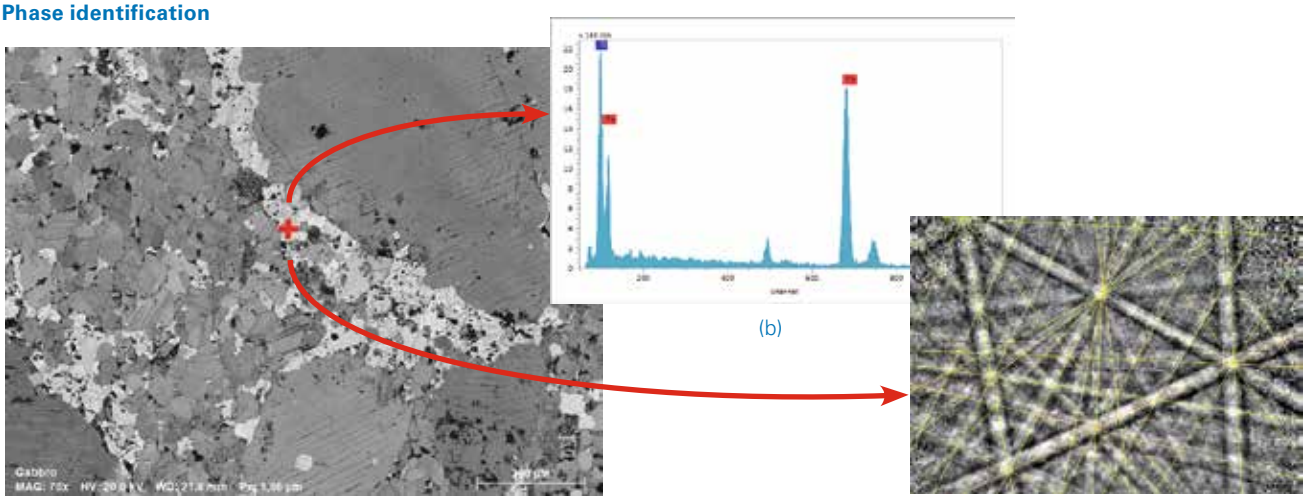

(a) (b) (c)

Fig. 2 (a) Pattern quality map (PQM, grayscale), (b) EDS spectrum from the point marked red on the map (a), (c) corresponding EBSP with indexed Kikuchi bands using the Advanced Phase ID result (magnetite).

3. Automatic (or interactive) band detection of the EBSP (Fig. 2c).

4. Subsequent automated software analysis is performed within five seconds to index the EBSP with the 384 candidate phases. Solutions are classified based on the quality of fit.

5. The best fitting phase file (magnetite) is added to the phase list.

Offline Advanced Phase ID

After measurement, both EDS and EBSD datasets are automatically saved in one file. It is not necessary to save diffraction patterns since Kikuchi band positions are automatically saved and generally provide sufficient information.

Using the ESPRIT software, the EDS information is extracted from the combined EBSD/EDS data into the HyperMap shown in Fig. 3. HyperMap is Bruker's data format used to illustrate the chemical distribution of the area using the full EDS spectrum at every pixel. The HyperMap is quantified for later EDS assisted indexing in order to distinguish phases of similar crystallography.

The identification of the remaining phases was performed offline in a similar manner as online. Either Kikuchi band positions or diffraction patterns can be used. The offline procedure is described in steps 6 – 9.

EDS HyperMap

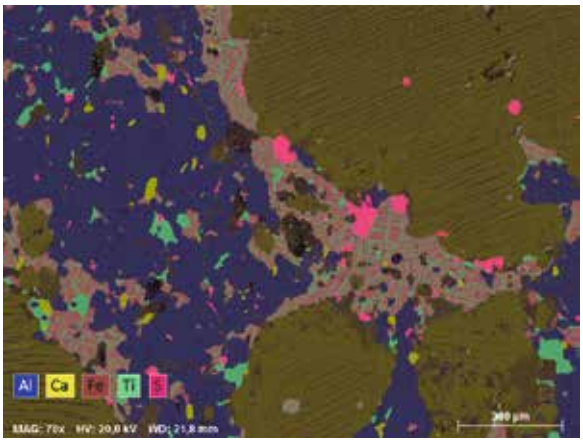

Fig. 3 EDS HyperMap showing the chemical distribution in the measured area. Note that the exsolution within the large grains is calcium deprived.

6. Using the Spot Mode feature, a point on the map is selected where no phase has been determined. The corresponding EDS and EBSD data are automatically displayed.

7. Carrying out Advanced Phase ID. The best fitting solution is added to the map phase list followed by ultrafast re-indexing.

8. Steps 6 and 7 must be repeated until all phases have been identified.

Unprocessed EBSD Phase distribution map

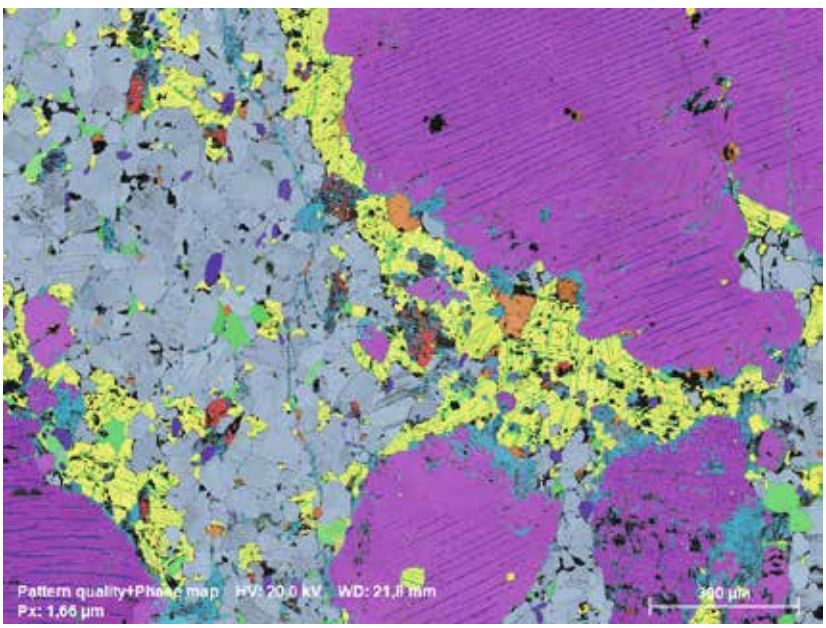

No.	Color	Phase name	IT no.	Space group	Crystal system
1		Magnetite	227	Fd3m(*)	cubic
2		Apatite-(CaOH)	176	$P6_3/m$	hexagonal
3		Pyrrhotite	194	$P6_3/mmc$	hexagonal
4		Quartz low	152	$P3_121$	trigonal
5		Ilmenite	148	R3	trigonal
6		Diopside	15	C2/c	monoclinic
7		Tremolite	12	C2/m	monoclinic
8		Clinohypersthene	14	$P2_1/c$	monoclinic
9		Clinochlore	2	P1	triclinic
10		Plagioclase	2	P1	triclinic

Fig. 4 PQM and unprocessed EBSD phase map revealing the completed phase distribution after Advanced Phase ID and re-indexing. The non-indexed points are displayed in black. The re-indexing procedure was combined with automatic EDS assisted phase discrimination in order to distinguish the fine clinohypersthene exsolutions within the coarse diopside grains.

Orientation distribution map

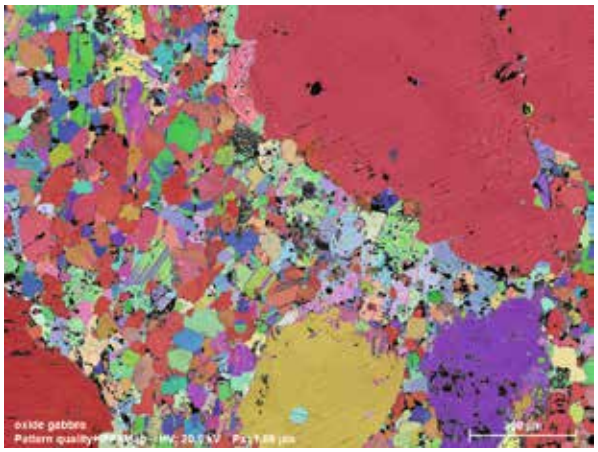

Fig. 5 PQM overlaid by orientation distribution (along tilt axis) to illustrate the performant indexing of ten phases.

9. Final step of the process is to re-index the whole map with the completed phase list. The speed of this process depends on the number of phases and their symmetries – e.g. in this example it was reindexed, with EDS assistance, at 355 points per second (pps) using a laptop.

Results

After reanalysis, the completed EBSD dataset is obtained as shown in Figs. 4 and 5. The completed map in Fig. 5 reveals the presence of 10 different crystallographic phases and a very high indexing hit rate of 95%. It illustrates the ability of the software to reliably index low and high crystal symmetry phases: magnetite (cubic); pyrrhotite and apatite (hexagonal); quartz and ilmenite (trigonal); clinochlore and plagioclase (triclinic); diopside, clinohypersthene, and tremolite (Ca-amphibole group), (monoclinic).

Most of the non-indexed points are associated with the porosity, which is very common in geologically formed samples. The complete identification of the mineral assemblage, including accessory phases, allows more accurate estimation of the sample's pressure-temperature-variations through time.

The presence of clinochlore (from the chlorite group) and tremolite (from the amphibole group) suggests a reaction with the surrounding metamorphic veins. Despite its poor diffraction pattern quality, the clinochlore phase was identified by Advanced Phase ID and successfully indexed afterwards.

It is important to note that out of the identified 10 phases 5 are of low symmetry: three monoclinic (diopside, clinohypersthene and tremolite) and two triclinic (clinochlore and plagioclase). Despite having similar crystallography, the robustness of ESPRIT's indexing algorithm has produced no misindexing between these phases (see Figs. 4 and 5). The completed EBSD map also confirms the presence of fine clinohypersthene exsolutions within the coarse diopside grains and both phases are discernible.

Conclusion

The QUANTAX EBSD system optimizes time spent at the SEM by conducting a measurement without necessarily knowing all present phases in the specimen. The dataset can be subsequently completed at any time, thanks to the Advanced Phase ID feature and ultrafast reanalysis using the ESPRIT software.

In the analyzed area of the mineralogical sample 10 different crystallographic phases were rapidly and accurately identified. The succesful characterization of such a complex sample was only possible through ESPRIT's state of the art pattern indexing algorithm combined with its automatic EDS assisted phase discrimination feature.

The ability to correctly identify all phases, including accessory ones and exsolutions, and to measure their orientations will contribute to the successful study of complex mineralogical samples.

Acknowledgements

The sample was obtained from IODP expedition 304/305, number 20144B (NERC grant code NE/D521549/1). The dataset was acquired at CSIRO Laboratory (Perth, Australia). The author would like to express her gratitude to Dr. A. Halfpenny from the Microscopy & Microanalysis Facility, John de Laeter Centre, Curtin University, Australia, for sharing the dataset and for the feedback on the sample and on this application note.

Author

Dr. Laurie Palasse, Application Scientist EBSD, Bruker Nano GmbH

Bruker Nano GmbH
Berlin · Germany
Phone +49 (30) 670990-0
Fax +49 (30) 670990-30
info.bna@bruker.com

www.bruker.com/quantax-ebsd